J. Phys. B: At. Mol. Opt. Phys. **30** (1997) 3897–3911. Printed in the UK PII: S0953-4075(97)83740-6

Photoionization–excitation of helium using an R-matrix with pseudostates method

T W Gorczyca† and N R Badnell‡

† Department of Physics, Western Michigan University, Kalamazoo, MI 49008-5151, USA

‡ Department of Physics and Applied Physics, University of Strathclyde, Glasgow G4 0NG, UK

Received 29 April 1997

Abstract. We have developed an alternative R-matrix with pseudostates (RMPS) method for incorporating a two-electron continuum description into the wavefunction of electron–ion collision calculations. This method is similar in spirit to various recent treatments of the pseudostate expansion, most notably the R-matrix approaches of Meyer and Greene, and Bartschat *et al*. Our approach differs in that we: (1) utilize a direct sum of several bases: the physical He^+ target orbitals, additional MCHF pseudo-orbitals for the He ground state, R-matrix continuum orbitals, and, on occasion, Laguerre orbitals, and (2) rely on a different approach for the creation of an orthonormal basis. Since we use the Belfast codes that are based on a Wigner–Eisenbud R-matrix treatment, we also need to introduce a modified Buttle correction. The method is first tested on the s-wave (Temkin–Poet) model for electron-impact excitation and ionization of He^+. Then it is applied to the calculation of cross sections and angular distributions for the photoionization–excitation process $h\nu + He(1s^2) \longrightarrow He^+(nl) + e^-$ $(n = 2, 3)$. We find that these results are greatly improved by the inclusion of the two-electron continuum description, which is more important for the ground state, but plays a role in the final photoionized states as well. A highly correlated multiconfiguration Hartree–Fock expansion is used to represent the ground state, and from the configuration interaction coefficients, asymptotic ratios σ_n/σ_1 are determined and compared with other theoretical results. Results are also compared with recent high-energy measurements for the $n = 2, 3$ cross section ratios and angular distribution parameters. This pseudostate expansion allows us to predict photo–double-ionization cross sections, $h\nu + He(1s^2) \longrightarrow 2e^-$. Of particular significance, we find good agreement between our length and velocity gauge results, indicating that our ground-state correlation is sufficiently converged for the present system.

1. Introduction

Recently, there has been a great revival of interest in photo–double-ionization. This is the process by which one photon incident on a helium atom leads to the ejection of two atomic electrons; helium is the obvious ideal system for the study of double ionization processes since it is the simplest multi-electron atom. McGuire *et al* (1995) reviewed the theoretical and experimental status of this field up until 1995, and a more detailed summary of various studies up until 1992 can be found in the review by Schmidt (1992). On the theoretical side, the treatment of this process poses a great challenge since it is necessary to describe properly a wavefunction that allows the escape of both target electrons from the atomic region.

Photoionization–excitation is a process similar to photo–double-ionization in that an incident photon causes the simultaneous ejection of one atomic electron and excitation (into a higher orbital nl, $n > 1$) of the other. In either case, two diffuse electron orbitals must be

0953-4075/97/173897+15$19.50 © 1997 IOP Publishing Ltd

described. Furthermore, the two competing processes may interfere with each other so that, for instance, photoionization–excitation may be strongly influenced by the neighbouring possibility of double ionization at higher energies, and vice versa. It can be said that polarization of the excitation process is influenced by the target continuum, similar to the early revelation that the continuum of the electron–proton system accounts for 18% of the static dipole polarizability of atomic hydrogen (Castillejo *et al* 1960). This discovery first had immediate and important implications in its application to electron-impact excitation.

One of the most successful and widely used numerical techniques for treating a system composed of a scattering electron plus a target atom or ion is the continuum Hartree–Fock method, most commonly implemented as the close-coupling approximation (Seaton 1953). The essential part in this method is that the complete wavefunction is expanded as a sum of product functions of the target and continuum electron wavefunctions. In general, a complete expansion for the radial wavefunction of a two-electron system takes the form

$$\Psi(r_1, r_2) = \left\{ \sum_i \Phi_i(r_1) f_i(r_2) + \int \mathrm{d}k\, \Phi(k, r_1) f(k, r_2) \right\} \tag{1}$$

$$\pm \left\{ \sum_i \Phi_i(r_2) f_i(r_1) + \int \mathrm{d}k\, \Phi(k, r_2) f(k, r_1) \right\}, \tag{2}$$

where Φ_i are, for the present case, bound hydrogenic wavefunctions for the He^+ ion, $\Phi(k)$ are positive energy Coulombic orbitals in the field of a $Z = +2e$ nucleus, and $f_i(f(k))$ are undetermined continuum orbitals for the incident electron. The $\pm$ arises from the required antisymmetrization of the problem, which depends on the orbital angular momentum and spin. The usual close-coupling expansion approximates this by neglecting the second integral term and reducing the (infinite) sum in the first term to a few 'target' states of interest. However, it has long been recognized that the standard implementation of this method cannot account for the target continuum states, since the (finite) sum over i only represents (a portion of) the bound spectrum of the He^+ ion. One approach for alleviating this restriction is to augment the sum over certain real target states with additional *pseudostates*, a strategy first applied to electron–atom systems by Burke *et al* (1969).

Recently, there have been marked improvements in computational facilities *and* theoretical methods to treat the target continuum. The convergent close-coupling (CCC) method of Bray and Stelbovics (1992) has proven to be quite successful at describing a variety of processes affected by the target continuum (Bray and Stelbovics 1995). They approximate the (momentum space) target continuum with a finite expansion of Laguerre orbitals. The success of the CCC method has prompted the extension of this pseudostate expansion to other (position space) close-coupling methods, in particular the R-matrix method. Meyer and Greene (1994) first extended these basic ideas within the eigenchannel R-matrix method. They represented the physical and pseudo-orbitals by an expansion in 'box' states for this system (orbitals with zero amplitude but, in general, non-zero derivative, at the R-matrix boundary). Thus, they demonstrated that the finite wavefunction expansion, properly modified to include discrete pseudostates in the continuum, could be meaningful and yield double ionization information. This was extremely important because it meant that computer codes developed over the years for the treatment of one-electron continuum processes in electron–atom (ion) collisions could be extended to treat the double continuum, at least in principle. Recently, Bartschat *et al* (1996a), utilizing a new development of the Belfast R-matrix codes (Burke and Berrington 1993), known as RMATRIX II (Burke *et al* 1994), have used this same essential idea in what they (and hereafter we) refer to as the R-matrix with pseudostates (RMPS) method. Their representation of the target continuum

is accomplished with a finite expansion of Sturmian orbitals. They have applied this method to electron collisions with hydrogen (Bartschat *et al* 1996b), helium (Bartschat *et al* 1996c), beryllium (Bartschat *et al* 1996d), and boron (Marchalant *et al* 1997). We note that this RMPS version of Bartschat *et al* (1996a) is not presently set up to treat photoionization processes.

In this study we will describe modifications to the latest RMATRIX I version of the Belfast codes (Berrington *et al* 1995) which can incorporate both Breit–Pauli and radiative (e.g. photoionization) effects, as originally developed by Scott and Taylor (1982). We have already used our method to treat electron-impact excitation (Badnell and Gorczyca 1997) and ionization (Pindzola *et al* 1997), but did not provide all of the numerical details, and did not study any photoionization processes. We realize that there are several alternative methods for treating two-electron continuum processes, such as the intermediate-energy *R*-matrix method (Burke *et al* 1987, Scott *et al* 1989), or the hyperspherical close-coupling method (Tang and Shimamura 1994), all with merit of their own. For this study, however, we are primarily concerned with features of the close coupling with pseudostates method in its application to photoionization processes.

Photoionization calculations, unlike electron-impact excitation calculations—which need only solve for the electron–ion scattering wavefunction—are further complicated by the need to describe the initial ground-state wavefunction accurately. It is absolutely essential to incorporate a high degree of interelectron correlation in the ground state in order to obtain reliable photoionization cross sections, particularly when attempting to converge results using different gauge forms of the dipole operator (Starace 1982, Schmidt 1992). The eigenchannel *R*-matrix approach, although used to treat electron-impact excitation and ionization within a model s-wave problem (Meyer *et al* 1995), was first applied to a study on photo–double-ionization of helium by Meyer and Greene (1994). They reported well behaved ionization cross sections in the velocity and acceleration gauges, but pointed out that their unreported length gauge calculations gave unreasonably large cross sections. We note that Meyer and Greene have subsequently converged results from all three gauges using finite element methods (Meyer *et al* 1997). The same difficulty in the length gauge was noted by Kheifets and Bray (1996), who did not report the length results either, but attributed these poorer results to a lack of convergence of the ground-state correlation. Thus, while there have been similar studies on photoionization including the target continuum, such questions as the unreliability of the length gauge within *R*-matrix calculations calls for further independent *R*-matrix studies.

Little attention has been paid to the similar process of photoionization–excitation. This process is interesting because it is also sensitive to final-state correlation, but many of the difficulties associated with ionization calculations are not present, most importantly the interpretation of excitation to pseudostates. Thus, it is an ideal process for investigating initial- and final-state correlation. Moreover, there have been recent measurements for both the angular distribution (Wehlitz *et al* 1993) and ratios (Wehlitz 1997) over an energy range of hundreds of volts, without a corresponding new theoretical investigation of the $n = 3$ states. Although excitation to the $n = 2$ state has received extensive theoretical study (Schmidt 1992), there has been very little investigation for the $n = 3$ state. To our knowledge, there is the standard *R*-matrix study of Hayes and Scott (1988) in the resonance region below the $n = 4$ threshold, and the many-body perturbation theory calculations of Salomonson *et al* (1989) for the $n = 2$ and $n = 3$ states, who cautioned that their $n = 3$ results 'are not to be considered very accurate'. This warrants a new theoretical investigation.

This paper is organized as follows. In section 2 we describe our new numerical methods

that allow us to use expanded basis sets to incorporate ground-state correlation and the target continuum. In particular, we present our new orthonormalization algorithm and the consequential need to modify the Buttle correction. In section 3 this alternative RMPS method is first applied to a simple s-wave scattering problem, the Temkin–Poet model. In section 4 we outline our basic strategy for investigating the higher-order photoionization processes for helium, including a description of our various orbital bases. In section 5 R-matrix results for photoionization–excitation using these bases, the analytic extension to asymptotically high energies, photo–double-ionization, and a comparison with experimental measurements are given, followed by our concluding remarks in section 6.

2. R-matrix with pseudostates method

The expansion for the spatial portion of the wavefunction within the standard application of the R-matrix method (Burke and Berrington 1993) takes the following form for our case:

$$\psi(r_1, r_2) = \left\{ \sum_{nll'} P_{nl}(r_1) \left[\sum_i b_{nl,il'} u_{il'}(r_2) + \sum_{n'} c_{nl,n'l'} P_{n'l'}(r_2) \right] \right\} \pm \left\{ \sum_{nll'} P_{nl}(r_2) \left[\sum_i b_{nl,il'} u_{il'}(r_1) + \sum_{n'} c_{nl,n'l'} P_{n'l'}(r_1) \right] \right\}. \tag{3}$$

The target orbitals $P_{nl}(r)$ are chosen to give an accurate representation of the ionic states, which in our case are hydrogenic states for the He^+ ion. The continuum orbitals are determined from the following differential equation:

$$\left(\frac{d^2}{dr^2} - \frac{l(l+1)}{r^2} + V(r) + k_{il}^2 \right) u_{il}(r) = \sum_n \lambda_{inl} P_{nl}(r), \tag{4}$$

where $V(r)$ is chosen so that the continuum orbitals give a good representation of the actual scattering orbital. The Lagrange multipliers on the right-hand side of equation (4) ensure that $\langle u_{il} | P_{nl} \rangle = 0$ (the bra-ket notation denotes integration over the R-matrix region), so that the combined basis of the $P_{nl}(r)$ and the $u_{il}(r)$ is orthonormal. However, a difficulty arises when using pseudo-orbitals to augment the target orbital basis. (We follow the practice of denoting these pseudo-orbitals by $\overline{P_{nl}}(r)$ to emphasize that they are not physical He^+ orbitals.) As has been previously noted (Burke and Robb 1975, Bartschat *et al* 1996a), it is more efficient and meaningful to omit the pseudo-orbitals from the right-hand side of equation (4), that is, to avoid Lagrange orthogonalizing the continuum orbitals $u_{il}(r)$ to the pseudo-orbitals. Their inclusion mimics an exchange effect which introduces unphysical behaviour in the continuum (Bartschat *et al* 1996a). Thus, in general, the continuum orbitals are not orthogonal to the pseudo-orbitals ($\langle u_{il} | \overline{P}_{nl} \rangle \neq 0$). In the implementation of Bartschat *et al* (1996a), the approach is to invoke the recursive Gram–Schmidt orthonormalization procedure to convert these continuum orbitals into a new set, $v_{il}(r)$, which, together with the physical and pseudo-orbitals, form an orthonormal set. However, this method can quickly become unstable as the number of pseudo-orbitals and/or continuum orbitals increases, and so they point out the need for further orthonormalization. The source of the instability can be understood by noting that when any of the pseudo-orbitals is nearly spanned by the resultant continuum orbital basis, $u_{il}(r)$, then eventually one will produce a 'nearly-zero' orbital in the orthogonalization, which is thus renormalized with an extremely large number (Stoer and Bulirsch 1980). We take a different approach, which we now describe, and find this method to be quite stable.

2.1. Generation of a stable, orthonormal basis

For the present RMPS implementation, it is necessary to generate an orthonormal basis of orbitals $v_{il}(r)$ from two distinct, overlapping bases. They are: (1) the physical orbitals $P_{nl}(r)$ plus the (orthogonal) pseudo-orbitals (MCHF or Laguerre) $\overline{P}_{nl}(r)$, and (2) the R-matrix continuum orbitals $u_{il}(r)$. The continuum orbitals are orthogonal to the physical orbitals (by using Lagrange multipliers) but, in general, overlap with the pseudo-orbitals and so we need to create a final orthonormal basis containing both sets. We represent our orbitals by the matrices $\overline{\mathbf{P}}$ and $\mathbf{U}$ so as to simplify the notation. The matrix elements for a given orbital angular momentum l are given by $(\mathbf{U})_{ij} = u_{il}(r_j)\sqrt{w_j}$. The orbitals are discretized onto radial mesh points r_j, so that any integral can be expressed as $\int u_{i'l}(r)u_{il}(r)\,\mathrm{d}r \approx \sum_j u_{i'l}(r_j)u_{il}(r_j)w_j \equiv (\mathbf{U}\mathbf{U}^{\mathbf{T}})_{i'i}$, where w_j are the weighting factors. Thus, all integrals between orbitals can be summarized by the three matrix equations

$$\overline{\mathbf{P}}\,\overline{\mathbf{P}}^{\mathbf{T}} = \mathbf{1}, \qquad \mathbf{U}\mathbf{U}^{\mathbf{T}} = \mathbf{1}, \qquad \mathbf{U}\overline{\mathbf{P}}^{\mathbf{T}} = \mathbf{M} \neq \mathbf{0}. \tag{5}$$

The last of these indicates that the combined basis of $\overline{\mathbf{P}}$ and $\mathbf{U}$ is not orthonormal, but instead involves an overlap matrix $\mathbf{M}$. We can express the direct sum of these two bases as follows

$$\mathbf{V} = \begin{pmatrix} \overline{\mathbf{P}} \\ \mathbf{A}\overline{\mathbf{P}} + \mathbf{B}\mathbf{U} \end{pmatrix}. \tag{6}$$

By demanding that $\mathbf{V}\mathbf{V}^{\mathbf{T}} = \mathbf{1}$, i.e. by generating an orthonormal basis of orbitals $v_{il}(r)$, we obtain the conditions

$$\mathbf{A} = -\mathbf{B}\mathbf{M}, \tag{7}$$

which is equivalent to the orthogonalization step in the standard Gram–Schmidt procedure, and

$$\mathbf{B}(\mathbf{1} - \mathbf{M}\mathbf{M}^{\mathbf{T}})\mathbf{B}^{\mathbf{T}} = \mathbf{1}, \tag{8}$$

which is equivalent to the renormalization step. We note that, up to this point, the procedure is identical to most methods for creating an orthonormal basis, for instance, the Gram–Schmidt orthonormalization procedure. Indeed, the early pseudostate work of Burke *et al* (1969) used a nearly identical formalism, detailed in their appendix. However, an obvious difficulty arises when the two bases are linearly dependent. (In theory, this cannot occur since the two sets of orbitals have different logarithmic derivatives at the R-matrix boundary, but in practice the numerical difference is negligible.) This linear dependence manifests itself by yielding a singular matrix $\mathbf{1} - \mathbf{M}\mathbf{M}^{\mathbf{T}}$, making it impossible to satisfy the second of the above conditions numerically. The different approach that we take is to diagonalize this matrix, $\mathbf{O}^{\mathbf{T}}(\mathbf{1} - \mathbf{M}\mathbf{M}^{\mathbf{T}})\mathbf{O} = \mathbf{d}$, with $\mathbf{d}$ diagonal, and then form the matrix $\mathbf{B} = \mathbf{d}^{-1/2}\mathbf{O}^{\mathbf{T}}$ *only for those rows with non-zero eigenvalue* (in practice we keep those with eigenvalues greater than 10^{-4}, which we find is sufficient to avoid numerical instability). In other words, this transformation avoids the linear dependence problems associated with the overlapping bases $\overline{\mathbf{P}}$ and $\mathbf{U}$ by retaining only the minimum set of spanning basis orbitals. These are determined solely by inspecting the eigenvalues of the matrix $\mathbf{1} - \mathbf{M}\mathbf{M}^{\mathbf{T}}$. While not a new numerical approach in principle, we have found that this procedure yields a stable basis of orbitals $v_{il}(r)$ for use, in conjunction with the physical orbitals $P_{nl}(r)$ and pseudo-orbitals $\overline{P}_{nl}(r)$, in our RMPS method. Thus, we can choose an arbitrarily large set of appropriate pseudo-orbitals of a varied nature. For instance, it is advantageous to include some pseudo-orbitals that accurately describe the initial state in photoionization and others that represent

the continuum of the target electron. For our case, a number of pseudo-orbitals and many continuum orbitals are required.

Another difficulty presented by a direct sum of overlapping bases is that the Buttle correction, an absolutely essential part required by the Wigner–Eisenbud (Belfast) R-matrix method so as to obtain reliable scattering information, requires modification when using the RMPS method. This is because the standard Buttle correction assumes that the original R-matrix basis $u_{il}(r)$ is used. When additional pseudo-orbitals are included, however, the Buttle correction must take these additional orbitals into consideration. Bartschat *et al* (1996a) avoided this difficulty by instead discarding high-energy R-matrix poles arising from these additional pseudo-orbitals, based on perfectly valid considerations of these poles (Bartschat 1996). We retain all poles and use a new Buttle correction, on the other hand, and feel that this approach may have certain advantages. For instance, there is no need to determine which R-matrix poles should be discarded.

2.2. New Buttle correction

The Buttle correction (Buttle 1967) is a nearly energy-independent correction, at sufficiently low energies, to the single-channel R-matrix given by the difference between the actual single-channel R-matrix and the approximate one arising from the use of a finite number of terms in the expansion of equation (2):

$$R_{\text{Buttle}} = R_{\text{actual}} - R_{\text{approx}}. \tag{9}$$

The actual R-matrix is computed by solving equation (4) at the Buttle energies, whereas the approximate R-matrix, in the absence of any pseudo-orbitals, is given by the expression (Burke and Berrington 1993)

$$R_{\text{approx}} = \frac{1}{2a}\vec{U}^{\mathsf{T}}(a)(\mathbf{H} - E)^{-1}\vec{U}(a). \tag{10}$$

Here $\mathbf{H}$ is the Hamiltonian matrix (the one-electron operator in equation (4)), which is diagonal when acting only on the basis $\mathbf{U}$. $\vec{U}(a)$ is the vector of surface amplitudes on the R-matrix boundary $r = a$, i.e. $(\vec{U}(a))_i = u_{il}(a)$. Thus, the Hamiltonian matrix $\mathbf{H}$ can be replaced by the diagonal matrix of eigenvalues, giving the simple R-matrix form

$$R_{\text{approx}} = \frac{1}{2a}\sum_i \frac{u_{il}^2(a)}{k_i^2/2 - E}. \tag{11}$$

The above simplification does not hold when pseudo-orbitals are included. The approximate single-channel R-matrix is instead given by

$$R_{\text{approx}} = \frac{1}{2a}\vec{V}^{\mathsf{T}}(a)(\mathbf{H} - E)^{-1}\vec{V}(a), \tag{12}$$

indicating that it is expressed in terms of the new basis $\mathbf{V}$. This is not diagonal in general since $\mathbf{V}$ contains an admixture of pseudo-orbitals, although it is easily proven that all of the eigenvalues and surface eigenvectors of equation (4) are recovered. Due to the additional pseudo-orbitals, though, there exist additional eigenvalues with non-zero surface eigenvectors. (All are non-zero in general since they are linear combinations of both the pseudo-orbitals *and* the R-matrix orbitals, which have non-zero amplitudes at the R-matrix boundary.) We find that consideration of these additional terms is absolutely necessary to obtain a meaningful Buttle correction. Using the original form we obtained completely unphysical results. Our modified approach avoids this catastrophic error and instead gives a smooth Buttle correction and physically meaningful cross sections.

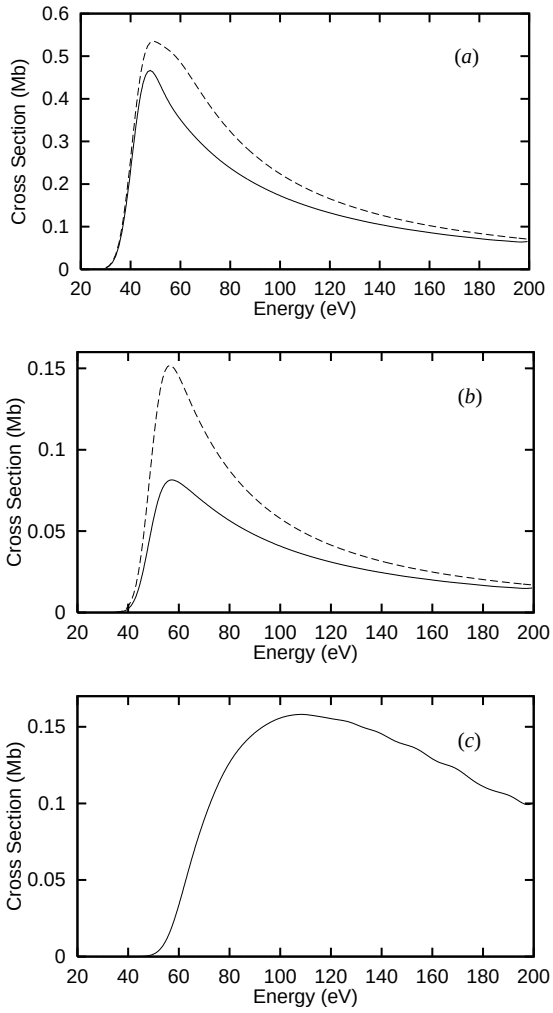

Figure 1. Standard R-matrix (– – –) and RMPS (——) results for $e^- + He^+$ collisions in the Temkin–Poet s-wave model: (*a*) 1s → 2s; (*b*) 1s → 3s; (*c*) 1s → ϵs. These represent sums over the singlet and triplet partial waves, and have been convoluted with a 10 eV FWHM Gaussian.

3. s-wave results for e^-–He^+ scattering: Temkin–Poet model

We first show that our method is valid by investigating the s-wave excitation and ionization cross sections for He^+. For this model system, we used physical orbitals for the $n = 1$–3 states, and an additional 12 Laguerre orbitals to discretize the continuum of the target electron. We also used 60 R-matrix orbitals for the continuum electron. The size of the wavefunction was thus of the order of 1000 basis functions (see equation (2)). Results are shown in figure 1 for excitation to the 2s and 3s states of He^+, and also ionization, obtained by summing the excitation cross sections to each target state with energy greater than the ionization energy (54.4 eV). The sum of singlet and triplet $L = 0$ partial waves is shown in each case, and they have been convoluted with a 10 eV FWHM Gaussian in order to smooth the sharp resonance structure, both physical and pseudo in nature, below each threshold.

The main points are, first, the results are completely consistent with those from a joint study using both the eigenchannel R-matrix and the convergent close-coupling methods (Meyer *et al* 1995) and also from a recent RMPS and CCC study (Bartschat and Bray 1997). However, the ionization results have not used any projection of pseudostates onto physical states, and further, none of the three results have done any sort of averaging over the R-matrix box size. Secondly, the standard R-matrix method gives an erroneously high excitation cross section due to the omission of higher channel coupling. Thus, the inclusion of the two-electron continuum is necessary even for excitation processes. Photoionization–excitation involves a similar wavefunction description for the final state, so it is natural to expect the two-electron continuum to be of similar importance there as well.

4. Details of our photoionization orbital bases

Applying the RMPS method to the photoionization of helium is complicated by the introduction of higher angular momentum orbitals. We need to include the $3d\epsilon f\,{}^1P^o$ continuum in order to study excitation up to $n = 3$, so all continuum orbitals up to $l = 3$ are needed. We require the hydrogenic orbitals $P_{nl} = \{1s, 2s, 2p, 3s, 3p, 3d\}$ to describe accurately the He^+ target states of interest. Since these alone would not be sufficient in order to obtain an accurate initial ground state for helium, we augment this set with an additional 12 orbitals $\overline{P}_{nl} = \{\overline{4s}, \overline{4p}, \overline{4d}, \overline{4f}, \overline{5s}, \overline{5p}, \overline{5d}, \overline{5f}, \overline{6s}, \overline{6p}, \overline{6d}, \overline{6f}\}$, determined from a large MCHF calculation (Froese Fischer 1991) for the ground state, including all 52 $nln'l$, $1 \leqslant n$, $n' \leqslant 6$, $0 \leqslant l \leqslant 3$ configurations. This yields a ground-state energy of $E = -2.903\,174$ au compared with the converged theoretical value of $-2.903\,724$ au (Froese Fischer 1977). These pseudo-orbitals thus recover a great deal of ground-state correlation, and they can be used to represent the continuum of the target electron as well. The He^+ energies obtained for these physical and pseudostates are given in table 1, showing that all of the higher target energies are in the continuum. The resultant discrete energy spectrum in the continuum is fairly sparse, however, and so the representation of the target continuum is correspondingly crude. In order to increase the density of states, we also tried to augment this pseudo-orbital basis with a set of Laguerre orbitals, similar to what was done for the Temkin–Poet model of scattering. This did very little to minimize the resulting oscillatory pseudoresonance structure, at a great increase in computational time and memory. Thus, we will not consider the use of Laguerre orbitals any further.

We use three basis sets for the calculations performed in section 5. For each set, the scattering electron orbital is spanned by the entire basis $\mathbf{V}$ consisting of physical, pseudo-, and R-matrix orbitals, as detailed in section 2.1. The three sets differ only in the number of target states included in the wavefunction of the initial (^1S) and final ($^1P^o$) partial waves. They are: basis (1) which includes only the six physical states in both initial and final partial waves, basis (2) which includes in addition the 12 pseudostates for the initial (^1S) partial wave, therefore allowing higher-order correlations not included in the standard R-matrix expansion, such as $\overline{4p}^2$, etc, and basis (3) which also includes 12 pseudostates in the final ($^1P^o$) partial wave, thus providing some representation for the double ionization wavefunction.

5. Photoionization–excitation results for helium

We started with the latest RMATRIX I version of the Belfast codes (Berrington *et al* 1995) that allow both Breit–Pauli and radiative (e.g. photoionization) effects, as originally

Table 1. Target energies for He^+.

He^+ designation[a]	Absolute (au)	Relative (Ryd)
1s	−2.00	0.00
2s	−0.50	3.00
2p	−0.50	3.00
3s	−0.22	3.55
3p	−0.22	3.55
3d	−0.22	3.55
$\overline{4s}$	0.22	4.44
$\overline{4p}$	0.51	5.01
$\overline{4d}$	1.59	7.17
$\overline{5s}$	3.02	10.04
$\overline{4f}$	3.87	11.74
$\overline{5p}$	4.69	13.38
$\overline{5d}$	8.80	21.60
$\overline{5f}$	15.26	34.51
$\overline{6s}$	15.74	35.48
$\overline{6p}$	20.79	45.58
$\overline{6d}$	32.03	68.05
$\overline{6f}$	47.05	98.10

[a] Those designated with an overline, e.g. $\overline{4s}$, are actually linear combinations of the original pseudo-orbitals

developed by Scott and Taylor (1982). These codes were then modified as detailed in section 2. We would like to investigate not only the differences between the results of the three bases described in section 4, but also the differences between theory and experiment. Experimentally, it is difficult to distinguish photoionization processes between He^+ target states with the same principal quantum number n, but different angular momenta l (Wehlitz *et al* 1993), due to the near degeneracy of hydrogenic targets; the measurable quantity usually involves a summation over all possible angular momentum states. We are therefore concerned with the following cross section ratios

$$R_n = \frac{\sigma_n}{\sigma_0} = \frac{\sum_{l=0}^{n-1} \sigma_{nl}}{\sigma_{1s}}, \tag{13}$$

where σ_{nl} are the individual cross sections to each nl state of He^+. This ratio is particularly useful in the present study because: (1) the experimental results have recently been reported (Wehlitz *et al* 1997); (2) the ratio approaches a constant, therefore factoring out much of the inverse-power energy dependence at high energies, and (3) the cross section to the ground state of He^+ (σ_{1s}) is found to be insensitive to the differences in our three R-matrix expansions, so that the ratio R_n essentially offers a concise assessment of the accuracy of our calculated photoionization–excitation cross sections. Results obtained using basis (1) (see figure 2) show a great disparity between length and velocity gauges as well as poor agreement with experiment. They are greatly improved in going to basis (2), indicating that the ground-state correlation is extremely important for these processes. However, even these results lie above experiment in the ionization threshold region (54.5 eV). The further final-state double-continuum description contained in basis (3) shows by far the closest agreement between the gauges and also seems to converge to the lower experimental results near the ionization threshold, although at the expense of introducing pseudoresonance oscillations.

We also computed effective angular distribution parameters (β). The normal angular

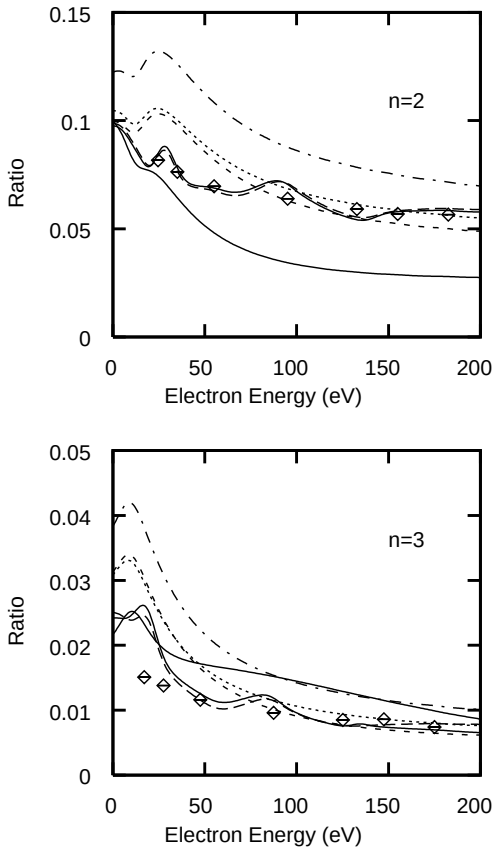

Figure 2. RMPS cross section ratios σ_n/σ_1 for He: basis (1), length (——) and velocity (— · —), basis (2), length (- - - -) and velocity (– – –), and basis (3), length (——) and velocity (— — —) results are all convoluted with a 10 eV FWHM Gaussian. The two (——) curves are easily differentiated by noting that the basis (1) length curve invariably shows the poorest overall behaviour compared with the others. Also, the length and velocity curves for basis (3) are often coincidental. The experimental values (◊) are from Wehlitz *et al* (1997).

distribution parameter is defined as the measure of anisotropy of the angular differential photoionization cross section, which is given by

$$\frac{\mathrm{d}\sigma_{nl}}{\mathrm{d}\Omega} = \frac{\sigma_{nl}}{4\pi}[1 + \beta_{nl} P_2(\cos\theta)], \tag{14}$$

where σ is the total integrated cross section, $P_2(\cos\theta)$ is the second-order Legendre polynomial, and θ is the angle between the axis of polarization of the incident, linearly polarized light and the ejected electron's wavevector. Again, since experiment cannot distinguish between β parameters of different l for the same n, we introduce an effective β parameter which averages over the l-states, namely

$$\beta_n^{\mathrm{eff}} = \frac{\sum_{l=0}^{n-1} \sigma_{nl}\beta_{nl}}{\sum_{l=0}^{n-1} \sigma_{nl}}. \tag{15}$$

We point out that when convoluting the effective β parameters we actually convolute the numerator and denominator separately and then take the quotient of the two convolutions. In figure 3 we show these results and note that, although they still exhibit some sensitivity to the two-electron continuum in the final state, this effect is reduced considerably from the corresponding effect for the ratios. This might be because β is essentially a ratio of two cross sections, and the errors in the numerator and denominator tend to cancel. However, it can be seen that the results from basis (3) show the least amount of difference between gauges and agree most closely with experiment. Also, the $n = 3$ length results from basis

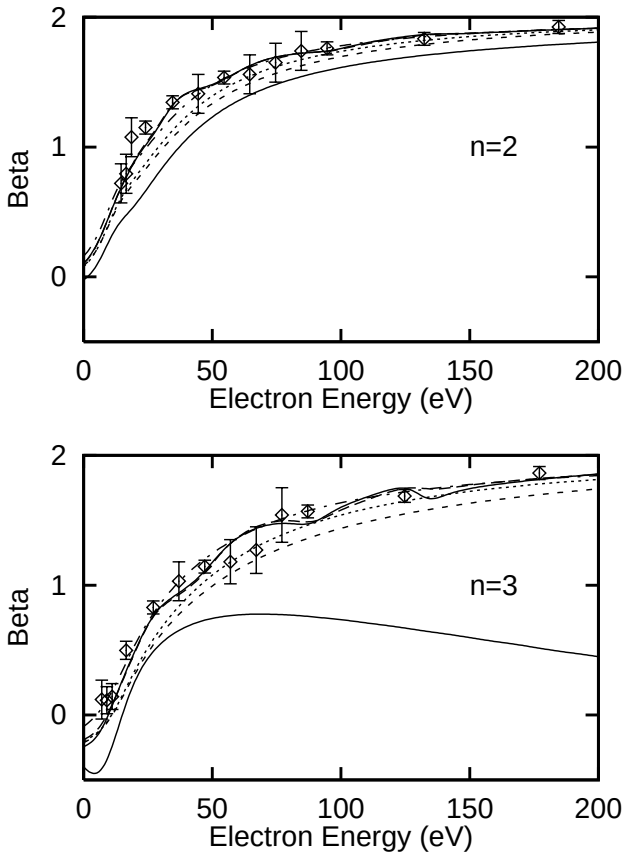

Figure 3. RMPS asymmetry parameters, β_n^{eff}, for He. Notation is the same as in figure 2. The experimental values (◊) are from Wehlitz *et al* (1993).

(1) are completely unphysical, again indicating that caution should be used when using approximate wavefunctions with the length gauge.

5.1. Analytic asymptotic limits

It is possible to extract the high-energy asymptotic limit for the cross section ratios from our ground-state wavefunction, with a minimal amount of work. The method of Åberg (1970), which was applied to velocity-gauge asymptotic ratios by Kheifets (1993), will be used here due to its simplicity. Our slightly different form for the ground-state wavefunction, including products of orbitals with $n \neq n'$,

$$\psi_g(r_1, r_2) = \sum_{n,l} \left\{ c_{nl,nl} P_{nl}(r_1) P_{nl}(r_2) \right. \tag{16}$$

$$\left. + \sum_{n' \neq n} \frac{c_{nl,n'l}}{\sqrt{2}} (P_{nl}(r_1) P_{n'l}(r_2) + P_{n'l}(r_1) P_{nl}(r_2)) \right\}, \tag{17}$$

necessitates an alternative form to that used by Kheifets (1993). Rigorously speaking, this expansion is modified slightly due to mixing with the extra R-matrix continuum orbitals,

Table 2. MCHF ground-state data.

n'	$c_{1s,n's}$	$c_{2s,n's}$	$c_{3s,n's}$	$P_{n'}(0)$
1	0.9618	−0.2223	−0.0738	5.657
2	−0.2223	−0.0112	−0.0072	2.000
3	−0.0738	−0.0072	−0.0023	1.089
4	−0.1211	−0.0179	−0.0086	6.671
5	0.0136	−0.0019	−0.0012	12.688
6	−0.0022	0.0011	0.0006	14.770

Table 3. Asymptotic ratios.

n	$\sigma_n E^2/A$	σ_n/σ_1 (%)	Kheifets (1993)
1	21.138		
2	1.014	4.80	4.74
3	0.125	0.59	0.60

although this is very minor since we have already included up through $n = 6$ pseudo-orbitals. One appealing aspect is that, since we use exact He^+ orbitals up to $n = 3$ in this expansion, there is no need to evaluate overlap integrals. Considering the alternative wavefunction and overlap, and following the analysis of Kheifets (1993), we arrive at the following expression for the asymptotic cross sections to the ns states of He^+ (the asymptotic cross section for a given n)

$$\sigma_n(E) \longrightarrow \frac{A}{E^2}\left| c_{ns,ns}P_{ns}(0) + \sum_{n' \neq n} \frac{1}{\sqrt{2}} c_{ns,n's}P_{n's}(0) \right|^2, \tag{18}$$

where the constant A is independent of n and the energy E. The MCHF coefficients and $r = 0$ orbital amplitudes are known prior to the R-matrix calculation, and we list these in table 2. Inspection of the size of the coefficients and amplitudes shows clearly that the 1s cross section is fairly insensitive to the effect of the $n > 3$ pseudo-orbitals; we can use just the $n = 1$–3 orbitals, slightly altering the mixing coefficients while still obtaining an asymptotic result that is accurate to within a few per cent. The mixing coefficients for the 3s cross section, on the other hand, are more sensitive to the amount of correlation included. The asymptotic ratios can be determined by using the data in table 2 and they are listed in table 3, showing that the present results are within about 2% of those of Kheifets (1993).

5.2. Analysis of the 3lnl' resonance region

We have primarily focused on energies above the ionization threshold, where no *physical* resonance structure is observed. However, we have seen that the background cross section is also affected by the two-electron description. This can be important for describing resonances that strongly interfere with the direct photoionization background.

An earlier study on resonant photoionization–excitation by Hayes and Scott (1988) used a standard R-matrix expansion including the $n = 4$ physical target states. They obtained impressive agreement with the positions and overall qualitative behaviour of the resonances seen in the $n = 2$ and $n = 3$ photoionization–excitation cross sections, although their calculated background (direct) cross section was considerably higher than experiment for certain processes. As analysed by Fano (1961), the relative magnitudes of direct and

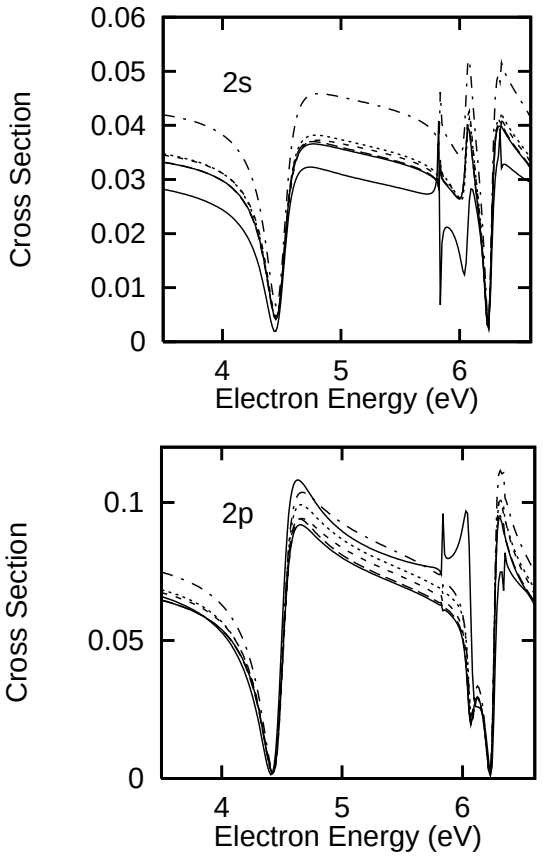

Figure 4. Unconvoluted photoionization–excitation cross sections σ_{2s} and σ_{2p} in the $3lnl'$ resonance region. Notation is the same as in figure 2.

resonant photoionization determine the resulting resonance profile (the Fano q-factor), which can range from infinity (Lorentzian) to order unity (asymmetric profile) to zero (window). The direct photoionization process must therefore be treated accurately, and we have seen that this is sensitive to the two-electron continuum description.

We show unconvoluted cross sections for photoionization–excitation to the 2s and 2p target states of He^+ in figure 4, using all three target bases. Of particular note, it is seen that the agreement between the length and velocity gauges improves as first the ground state, and then the final continuum state, each includes additional pseudostates in the wavefunction description. Furthermore, the background cross sections are reduced as well. Without the extra ground-state correlation, both the length and velocity results differ greatly, giving completely contrary qualitative descriptions for these resonances.

5.3. Double ionization calculations

Photo–double-ionization cross sections have already been computed with close-coupling methods by Meyer and Greene (1994) and Kheifets and Bray (1996). Nevertheless, this information is readily available from our present R-matrix calculations, and can be obtained by summing the photoionization cross sections to every pseudostate. These results are shown in figure 5. We note that Meyer and Greene (1994), Meyer *et al* (1996), and Bartschat *et al* (1996), have devoted considerable effort to the interpretation of excitation to pseudostates, which we do not attempt to repeat. The point we wish to make is that this method will

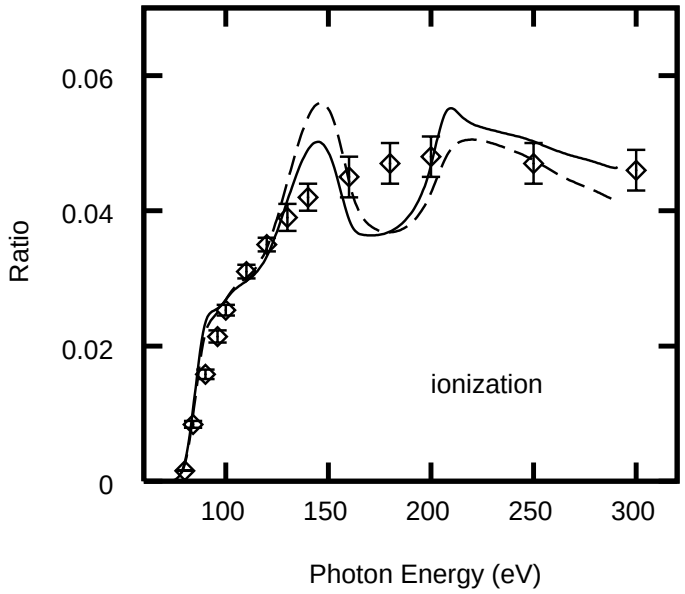

Figure 5. RMPS ratio of double-to-single ionization in He. Notation is the same as in figure 2. The experimental values (◊) are from Bizau and Wuilleumier (1995).

yield fairly accurate pseudostate double ionization cross sections via excitation to the target continuum states, as we have found in the case of electron-impact ionization (Pindzola *et al* 1997). In addition, we find good agreement between our length and velocity results, unlike the unreliable length gauge findings of Meyer and Greene (1994) and Kheifets and Bray (1996). As pointed out by Kheifets and Bray (1996), the length gauge is most likely to be extremely sensitive to the long-range behaviour of the ground-state wavefunction. Apparently, our MCHF pseudostate expansion, together with the extra R-matrix orbitals, minimizes the inaccuracy in the long-range behaviour of our ground state.

6. Conclusion

We have successfully developed an RMPS method which is able to handle a mixture of different, overlapping, orbital bases and which uses a modified Buttle correction. This method gave results for electron-impact excitation and ionization within the Temkin–Poet model that are consistent with those of other workers. The method was then applied to photoionization–excitation of He. It was found that a large MCHF expansion in pseudo-orbitals was necessary, in the form of double-continuum states for the ground state, to obtain reliable length and velocity results, therefore warranting this new development. Furthermore, the double-continuum states for the final scattering symmetry improved upon these results, and also yielded information on photo-double–ionization. Our accurate ground state produced asymptotic ratios in excellent agreement with other calculations. Most importantly, even the low-energy resonances were sensitive to the double-continuum description.

Acknowledgment

TWG would like to thank K Bartschat for useful discussions concerning the Belfast RMPS method.

References

Åberg T 1970 *Phys. Rev.* A **2** 1726
Badnell N R and Gorczyca T W 1997 *J. Phys. B: At. Mol. Opt. Phys.* **30** 2011
Bartschat K 1996 Private communication
Bartschat K and Bray I 1997 *Phys. Rev.* A **55** 3236
Bartschat K, Burke P G and Scott M P 1996d *J. Phys. B: At. Mol. Opt. Phys.* **29** L769
Bartschat K, Hudson E T, Scott M P, Burke P G and Burke V M 1996a *J. Phys. B: At. Mol. Opt. Phys.* **29** 115
——1996b *J. Phys. B: At. Mol. Opt. Phys.* **29** 2875
——1996c *Phys. Rev.* A **54** R998
Berrington K A, Eissner W B and Norrington P H 1995 *Comput. Phys. Commun.* **92** 290
Bizau J M and Wuilleumier F J 1995 *J. Electron Spectrosc. Relat. Phenom.* **71** 205
Bray I and Stelbovics A T 1992 *Phys. Rev.* A **46** 6995
——1995 *Adv. At. Mol. Phys.* **35** 209
Burke P G and Berrington K A 1993 *Atomic and Molecular Processes: An R-matrix Approach* (Bristol: IOP)
Burke P G, Burke V M and Dunseath K M 1994 *J. Phys. B: At. Mol. Opt. Phys.* **27** 5341
Burke P G, Gallaher D F and Geltman S 1969 *J. Phys. B: At. Mol. Phys.* **2** 1142
Burke P G, Noble C J and Scott M P 1987 *Proc. R. Soc.* A **410** 289
Burke P G and Robb W D 1975 *Adv. At. Mol. Phys.* **11** 143
Buttle J A 1967 *Phys. Rev.* **160** 719
Castillejo L, Percival I C and Seaton M J 1960 *Proc. R. Soc.* A **254** 259
Fano U 1961 *Phys. Rev.* **124** 1866
Froese Fischer C 1977 *The Hartree–Fock Method for Atoms* (New York: Wiley)
——1991 *Comput. Phys. Commun.* **64** 369
Hayes M A and Scott M P 1988 *J. Phys. B: At. Mol. Opt. Phys.* **21** 1499
Kheifets A S 1993 *J. Phys. B: At. Mol. Opt. Phys.* **26** L641
Kheifets A S and Bray I 1996 *Phys. Rev.* A **54** R995
Marchalant P J, Bartschat K, Berrington K A and Nakzaki S 1997 *J. Phys. B: At. Mol. Opt. Phys.* **30** L279
McGuire J H, Berrah N, Bartlett R J, Samson J A R, Tanis J A, Cocke C L and Schlachter A S 1995 *J. Phys. B: At. Mol. Opt. Phys.* **28** 913
Meyer K W and Greene C H 1994 *Phys. Rev.* A **50** R3573
Meyer K W, Greene C H and Bray I 1995 *Phys. Rev.* A **52** 1334
Meyer K W, Greene C H and Esry B D 1997 *Phys. Rev. Lett.* **78** 4002
Pindzola M S, Robicheaux F, Badnell N R and Gorczyca T W 1997 *Phys. Rev.* A at press
Salomonson S, Carter S L and Kelly H P 1989 *Phys. Rev.* A **39** 5111
Schmidt V 1992 *Rep. Prog. Phys.* **55** 1483
Scott M P, Scholz T T, Walters H R J and Burke P G 1989 *J. Phys. B: At. Mol. Opt. Phys.* **22** 3097
Scott N S and Taylor K T 1982 *Comput. Phys. Commun.* **25** 349
Seaton M J 1953 *Proc. R. Soc.* A **218** 400
Starace A F 1982 *Corpuscles and Radiation in Matter (Encyclopedia of Physics XXXI)* ed W Mehlhorn (Berlin: Springer) pp 1–121
Stoer J and Bulirsch R 1980 *Introduction to Numerical Analysis* (New York: Springer) p 197
Tang J-Z and Shimamura I 1994 *Phys. Rev.* A **50** 1321
Wehlitz R, Langer B, Berrah N, Whitfield S B, Viefhaus J and Becker U 1993 *J. Phys. B: At. Mol. Opt. Phys.* **26** L783
Wehlitz R *et al* 1997 *J. Phys. B: At. Mol. Opt. Phys.* **30** L51